

Increased Phosphorylation of Histone H1 in Mouse Fibroblasts Transformed with Oncogenes or Constitutively Active Mitogen-activated Protein Kinase Kinase*

(Received for publication, May 10, 1995, and in revised form, June 12, 1995)

Deborah N. Chadee‡§, William R. Taylor‡¶, Robert A. R. Hurta‡, C. David Allis¶, Jim A. Wright‡§, and James R. Davie§**

From the ‡Manitoba Institute of Cell Biology, University of Manitoba, Winnipeg, Manitoba, R3E 0V9 Canada, the §Department of Biochemistry and Molecular Biology, University of Manitoba, Winnipeg, Manitoba, R3E 0W3 Canada, and the ¶Department of Biology, Syracuse University, Syracuse, New York 13244-1270

We compared the nucleosomal organization, histone H1 subtypes, and histone H1 phosphorylated isoforms of *ras*-transformed and parental 10T½ mouse fibroblasts. In agreement with previous studies, we found that *ras*-transformed mouse fibroblasts have a less condensed chromatin structure than normal fibroblasts. *ras*-transformed and parental 10T½ cells had similar amounts of H1 subtypes, proteins that have a key role in the compaction of chromatin. However, labeling studies with ^{32}P and Western blot experiments with an antiphosphorylated H1 antibody show that interphase *ras*-transformed cells have higher levels of phosphorylated H1 isoforms than parental cells. G_1/S phase-arrested *ras*-transformed cells had higher amounts of phosphorylated H1 than G_1/S phase-arrested parental cells. Mouse fibroblasts transformed with *fes*, *mos*, *raf*, *myc*, or constitutively active mitogen-activated protein (MAP) kinase kinase had increased levels of phosphorylated H1. These observations suggest that increased phosphorylation of H1 is one of the consequences of the persistent activation of the mitogen-activated protein kinase signal transduction pathway. Indirect immunofluorescent studies show that phosphorylated H1b is localized in centers of RNA splicing in the nucleus, suggesting that this modified H1 subtype is complexed to transcriptionally active chromatin.

Due to their role in chromatin compaction, H1 histones are considered as general repressors of transcription (Weintraub, 1984). However, H1 histones are associated with transcriptionally active chromatin (Ericsson *et al.*, 1990; Kamakaka and Thomas, 1990). Both nucleosomes and H1 are present in the coding regions of active genes, but both are absent in the promoter (Nacheva *et al.*, 1989; Postnikov *et al.*, 1991; Belikov *et al.*, 1993). It is currently thought that the H1 interacts

differently with active and repressed chromatin (Garrard, 1991; van Holde *et al.*, 1992).

The H1 histones are a heterogeneous group of several subtypes that differ in amino acid sequence (Cole, 1987; Lennox and Cohen, 1988a; Parseghian *et al.*, 1994a). The relative amounts of H1 subtypes vary with cell type within a particular species, as well as among various species. For example, mouse tissues contain various levels of H1 subtypes, H1a, H1b, H1c, H1d, H1e, and H1⁰ (Lennox and Cohen, 1983). Since H1 subtypes differ in their abilities to condense DNA and chromatin fragments, it has been proposed that the differential distribution of the H1 subtypes with chromatin domains may generate chromatin regions with different degrees of compaction (Cole, 1987; Lennox and Cohen, 1988a). Indirect immunofluorescence studies with H1 subtype-specific antibodies have shown that the nuclear location of specific H1 subtypes is non-uniform. Rodent histone H1⁰ colocalized with nucleoli, human H1-3 is found primarily in the nuclear periphery, and human H1-1 is distributed in parallel to the DNA concentration (Gorka *et al.*, 1993; Breneman *et al.*, 1993; Parseghian *et al.*, 1993; Parseghian *et al.*, 1994b). Antibodies to human H1-2 and H1-4 generated a punctate staining pattern, reminiscent of the speckled staining patterns described when the nuclear sites of splicing factors, small nuclear RNAs, and RNA synthesis were localized (Parseghian *et al.*, 1994b; Huang and Spector, 1992; Jackson *et al.*, 1993; Lu *et al.*, 1994).

Further heterogeneity in the H1 population arises from post-translational modification. The H1 histones are phosphorylated at serine and threonine residues located in the N- and C-terminal domains of the protein (van Holde, 1988). Immunological and biochemical data show that H1 phosphorylation increases dramatically as cells progress through the cell cycle (Lu *et al.*, 1994; Hohmann, 1983). Phosphorylation of H1 begins in G_1 , continues at an increasing rate and extent throughout S and G_2 , and reaches a maximum in mitosis. The H1 subtypes, however, differ in their extent of phosphorylation and the scheduling of some of their phosphorylation during the cell cycle (Hohmann, 1983).

Phosphorylation of the H1 subtypes is likely to influence their interaction with DNA and, in turn, modulate chromatin structure (Hill *et al.*, 1990; Roth and Allis, 1992). It has been proposed that H1 phosphorylation drives chromosome condensation during mitosis (Bradbury, 1992). However, recent studies indicate that chromosome condensation can occur in the absence of H1 (Ohsumi *et al.*, 1993), and that other non-H1 chromosome-associated polypeptides play an important role in this process (Hirano and Mitchison, 1994). Reconstitution studies of chromatin with rat thymus H1 or phosphorylated H1, which was phosphorylated *in vitro* by p34^{cdc2} kinase to an

* This work was supported by Grant MA-12283 from the Medical Research Council of Canada (to J. A. W. and J. R. D.) and by Public Health Service Grant GM 40922 from the National Institutes of Health (to C. D. A.). The award of a Cancer Research Society, Inc. Studentship (to W. R. T.), a National Cancer Institute of Canada Terry Fox Senior Scientist (to J. A. W.) and a Medical Research Council Scientist (to J. R. D.) are also gratefully acknowledged. The costs of publication of this article were defrayed in part by the payment of page charges. This article must therefore be hereby marked "advertisement" in accordance with 18 U.S.C. Section 1734 solely to indicate this fact.

† Current address: Dept. of Molecular Biology, Cleveland Clinic Foundation, Cleveland, OH 44195.

** To whom correspondence and reprint requests should be addressed: Dept. of Biochemistry and Molecular Biology, Faculty of Medicine, University of Manitoba, Winnipeg, MB, R3E 0W3 Canada. Tel.: 204-783-3369; Fax: 204-783-0864.

average of 5.3 phosphates per molecule, showed that phosphorylation of H1 did not induce a condensation of chromatin structure. Instead, H1 phosphorylation caused a destabilization of chromatin structure at low ionic strength (Kaplan *et al.*, 1984). Another example of where H1 phosphorylation appears to have a function in the decondensation, rather than the condensation, of chromatin is with the *Tetrahymena* H1. H1 of *Tetrahymena* macronuclei, which are transcriptionally active, is highly phosphorylated. *Tetrahymena* H1 is completely dephosphorylated during conjugation when transcription ceases and chromatin becomes condensed (Lin *et al.*, 1991). Based upon these (and other) examples, it has been proposed that phosphorylation of H1 acts as a first step mechanism for inducing chromatin decondensation enabling access of factors for gene activation or replication as well as chromosome condensation (Roth and Allis, 1992).

Laitinen *et al.* (1990) observed that *ras*-transformed mouse (NIH-3T3) fibroblasts had a more decondensed nucleosomal structure than normal fibroblasts. Such an alteration in chromatin structure could be a result of alterations in H1 subtype levels or increased amounts of phosphorylated H1. In this report, we show that *ras*-transformed mouse fibroblasts have higher levels of phosphorylated isoforms of H1 subtypes b and c than the parental cells. Furthermore, mouse fibroblasts that were transformed with oncogenes (*raf*, *fes*, *mos*, or *myc*), most of which impact on the mitogen-activated protein (MAP)¹ kinase signal transduction pathway, had higher levels of phosphorylated H1 than the parental cell line (Davis, 1993; Blumer and Johnson, 1994; Hunter and Pines, 1994). Kinases involved in this pathway are MAP kinase kinase and MAP kinase. We show that NIH-3T3 cells transformed by a constitutively activated MAP kinase kinase have a greater level of phosphorylated H1 than the parental cells. These data suggest that the persistent activation of the MAP kinase pathway, which is thought to have a role in oncogenesis, leads to elevated amounts of the phosphorylated H1. In indirect immunofluorescence studies with an antibody to phosphorylated H1b, we observed a punctate pattern of nuclear staining in parental cells. This pattern of staining was also found in the *ras*-transformed cells. Furthermore, in both parental and *ras*-transformed cells, phosphorylated H1b co-localized to centers for RNA splicing.

MATERIALS AND METHODS

Cell Lines and Culture Conditions—The cell lines Ciras-2 and Ciras-3 were derived from 10T½ cells by transfection with the T24 Ha-ras oncogene (Egan *et al.*, 1987a). The NIH-3T3 mouse fibroblast cell lines transformed with human *c-myc*, *v-mos*, *v-fes*, or *A-raf* were NIH/hmyc1, Mos 1, Fes 1, and NIH/9IV#5, respectively (Egan *et al.*, 1987b). NIH-3T3 mouse fibroblasts cell lines transfected with inactive MAP kinase kinase or transfected and transformed with constitutively active MAP kinase kinase were K97M and ΔN3S222D, respectively (Mansour *et al.*, 1994; a gift from Drs. Natalie Ahn and Sam Mansour).

Cell lines were grown in plastic tissue culture plates in a humidified atmosphere containing 7% CO₂ in medium supplemented with penicillin G (100 units/ml) and streptomycin sulfate (100 µg/ml). The *ras*-transformed cell lines Ciras-2 and Ciras-3 and NIH-3T3 derived cell lines were grown in α-minimal essential medium plus 10% fetal bovine serum (Intergen, Purchase, NY). The proportion of cells in the different cell cycle phases was determined by fluorescent-activated cell sorting (Blosmanis *et al.*, 1987).

Isolation of Nuclei and Micrococcal Nuclease Digestion—All steps were performed on ice unless otherwise stated. The cell pellets were resuspended in 5 ml of TMN lysis buffer (10 mM Tris-HCl, pH 8.0, 100 mM NaCl, 300 mM sucrose, 2 mM MgCl₂, 1% thioglycol, 1 mM PMSF) using a glass Dounce homogenizer and glass pestle B. The suspension

was made 0.5% (v/v) Triton X-100 and passed through a 22-gauge needle three times. The nuclei were collected by centrifugation at 1000 rpm in a SS-34 rotor for 6 min. The pellet was resuspended in 5 ml of TMN lysis buffer and then the nuclei were collected by centrifugation. The nuclei were resuspended in digestion buffer (10 mM Tris-HCl, pH 8.0, 50 mM NaCl, 300 mM sucrose, 3 mM MgCl₂, 1% thioglycol, and 1 mM PMSF) to 9.5 A₂₆₀ units/ml. The DNA concentration of the nuclear suspension was determined as described previously (Delcuve and Davie, 1989). The suspension of nuclei was incubated at 37 °C. CaCl₂ was added to 1 mM followed by the addition of micrococcal nuclease to 15 A₂₆₀ units/ml. At various times of incubation, an aliquot was removed, and the digestion was terminated by placing the sample on ice and adding EDTA (pH 7.5) to 20 mM. To check for possible endogenous nuclease activity, nuclei were incubated in digestion buffer with CaCl₂ for the entire length of the experimental incubation period (mock digestion). Further, nuclei resuspended in digestion buffer were also stored on ice in the presence of EDTA, but in the absence of CaCl₂ and micrococcal nuclease.

Isolation of DNA and Electrophoresis of DNA Fragments—DNA extractions were carried out as described previously (Delcuve and Davie, 1989), except that the samples were incubated with SDS instead of sodium N-dodecyl sarcosine and proteinase K instead of Pronase. The nucleosomal organization of the nuclear DNA was analyzed by electrophoresis in 1% agarose gels (Delcuve and Davie, 1989). The negatives of the photographed gels were scanned with a PDI 325oe scanning densitometer, and the data were analyzed with ImageMaster 1D software.

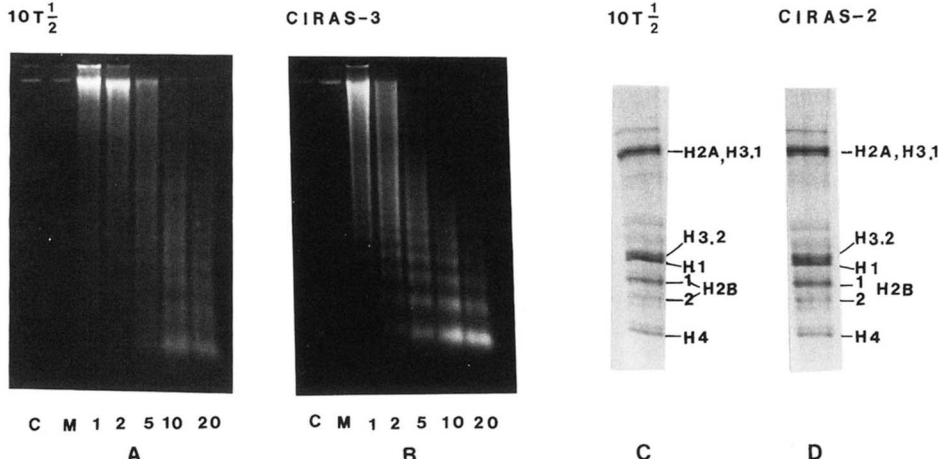
Isolation of Histones—For the isolation of histones, 5 × 10⁵ cells were plated per 150-mm plate, grown in 8% calf serum in α-minimal essential medium, and harvested 72 h later by trypsinization. Approximately 4 × 10⁷ to 1 × 10⁸ cells were used for histone preparation. Harvested cells were washed twice with PBS and homogenized in a glass homogenizer in 5 ml of nuclear preparation buffer (10 mM Tris-HCl, pH 7.6, 150 mM NaCl, 1.5 mM MgCl₂, 0.65% Nonidet P-40, and 1 mM PMSF). Nuclei were recovered by centrifugation at 1500 × g for 10 min. All centrifugations were carried out at 4 °C. Nuclei were resuspended in 3 ml of RSB buffer (10 mM Tris-HCl, pH 7.5, 3 mM MgCl₂, 10 mM NaCl, and 1 mM PMSF). To isolate H1, nuclei were extracted with 5% perchloric acid (Davie and Delcuve, 1991). For some experiments, cells were extracted directly with 5% perchloric acid, or nuclei were extracted with 0.4 N H₂SO₄ and then extracted with 5% perchloric acid (Davie *et al.*, 1987). The perchloric acid precipitate contained the nucleosomal histones. Protein concentration of histone samples was determined by the standard Bio-Rad protein assay (Bio-Rad Laboratories).

Metabolic Labeling of H1—Metabolic labeling was carried out as described previously (Yasuda *et al.*, 1981). Briefly, 2.5 × 10⁶ cells (per 150-mm plate) were grown for 24 h. The monolayers were washed twice with PBS, and then 5 ml of phosphate-free α-minimal essential medium containing 100 µCi/ml orthophosphate ³²P was added. Cells were incubated for 2 h, trypsinized, and then washed twice with PBS. H1 was isolated as described above. ³²P-labeled H1 was separated by SDS-15% polyacrylamide gel electrophoresis as described below, and dried gels were exposed to film.

Electrophoresis, Western Blotting, and Indirect Immunofluorescence Analyses—Proteins were analyzed by AUT (acetic acid, 6.7 M urea, 0.375% (w/v) Triton X-100)-15% polyacrylamide gels, SDS-15% polyacrylamide gels, and two-dimensional gel electrophoresis (AUT into SDS) (Nickel *et al.*, 1987; Davie, 1982). The gels were stained with Coomassie Blue. Histones separated by electrophoresis were transferred to nitrocellulose membranes as described (Delcuve and Davie, 1992). Antiphosphorylated H1 IgG was isolated as described by Lu *et al.* (1994). B1C8 monoclonal antibody was a gift from Dr. Jeffrey Nickerson and Dr. Sheldon Penman (Wan *et al.*, 1994). The membrane containing H1 was immunochimically stained with the antiphosphorylated H1 IgG and goat anti-rabbit antibody linked to horseradish peroxidase (Sigma) using the ECL (enhanced chemiluminescence) detection system (Amersham). For detection of the B1C8 antigen in total cellular protein from 10T½ cells, the membrane was stained with B1C8 monoclonal antibody and goat anti-mouse antibody linked to horseradish peroxidase using the ECL detection system. To quantitate the relative amount of phosphorylated H1b in each sample, we first prepared a Western blot that contained increasing amounts of Ciras-2 H1. The resulting autoradiogram was scanned, and the values obtained were linear up to 5 µg of Ciras-2 H1 histones. For each film, this procedure was repeated to ensure that the value (i.e. level of phosphorylated H1b) obtained with each preparation of H1 was in the linear range. Identical amounts of protein were loaded onto a SDS-15% polyacrylamide gel. The Coomassie Blue-stained gel pattern was scanned to obtain the relative amount of the H1 subtypes in each H1 sample. A standard

¹ The abbreviations used are: MAP, mitogen-activated protein; PMSF, phenylmethylsulfonyl fluoride; PIPES, 1,4-piperazinediethanesulfonic acid.

FIG. 1. Nucleosomal organization and histone composition of chromatin of *ras*-transformed and parental mouse fibroblasts. Mouse fibroblast 10T $\frac{1}{2}$ (A) or Ciras-3 (B) nuclei at 0.27 or 0.34 mg of DNA/ml, respectively, were digested with micrococcal nuclease for various times (minutes, indicated at the bottom of the figure). DNA fragments (10T $\frac{1}{2}$, 15 μ g; Ciras-3, 20 μ g) were resolved on 1% agarose gels which were stained with ethidium bromide. The cell cycle distribution of the cells used in this analysis was as follows: G₁, 48.2 (47.1); S, 22.8 (23.6); G₂/M, 29.0 (29.3) for 10T $\frac{1}{2}$ (Ciras-3). C and D, histones (10 μ g) isolated from nuclei of 10T $\frac{1}{2}$ (C) and Ciras-2 (D) were electrophoretically resolved on AUT-15% polyacrylamide gels. The Coomassie Blue-stained gels are shown.



curve was also generated by loading various amounts of Ciras-2 H1. The loading of each H1 sample was then corrected by dividing the amount of phosphorylated H1b (the value from the scanned autoradiogram) by the amount of total H1b (sum of H1b and c-phosphorylated histone H1b on Coomassie Blue-stained SDS gel pattern). The relative increase in phosphorylated H1b in each of the H1 preparations isolated from the oncogene- or MAP kinase kinase-transformed cell lines was divided by the value obtained for the parental cell line (10T $\frac{1}{2}$ or NIH-3T3). Indirect immunofluorescence was carried out as described previously (Lu *et al.*, 1994). Alternatively, before fixation with formaldehyde, cells were extracted with cytoskeletal buffer (10 mM PIPES, pH 6.8, 100 mM NaCl, 300 mM sucrose, 3 mM MgCl₂, 1 mM EGTA, 1.2 mM PMSF) containing 0.5% (v/v) Triton X-100 for 7 min at 4 °C to remove soluble proteins (Wan *et al.*, 1994; Durfee *et al.*, 1994). Colocalization of phosphorylated H1b with the B1C8 nuclear matrix antigen was done by mixing both primary antibodies, antiphosphorylated H1b and B1C8 monoclonal antibodies, followed by goat anti-rabbit IgG (fluorescein isothiocyanate) and goat anti-mouse IgM (Texas red; Jackson ImmunoResearch Laboratories, Inc.).

RESULTS

***ras*-Transformed Mouse Fibroblasts Have a More Decondensed Chromatin Structure Than Parental Cells—*ras*-transformed 10T $\frac{1}{2}$ fibroblast cell lines Ciras-3 and Ciras-2 are tumorigenic and highly metastatic (Egan *et al.*, 1987a). The nucleosomal organization of Ciras-3 cells was compared to that of the nontumorigenic and nonmetastatic parental mouse fibroblasts. Nuclei isolated from *ras*-transformed (Ciras-3) and parental 10T $\frac{1}{2}$ mouse fibroblasts were incubated with micrococcal nuclease, and the DNA fragments were resolved on agarose gels (Fig. 1). The nuclear DNA of *ras*-transformed (Ciras-3) cells was processed to mono- and dinucleosome sized DNA fragments at a rate 2.2-fold greater than that observed for the chromatin of parental cells. Nuclear DNA of Ciras-2 cells was digested at a rate similar to the chromatin of Ciras-3 cells (not shown). Ciras-3, Ciras-2, and 10T $\frac{1}{2}$ nuclei had very low levels of endogenous nuclease activity (see Fig. 1, lane M). Micrococcal nuclease digested DNA was also analyzed from NIH-3T3 cells and *c-myc*-transformed NIH-3T3 cells (cell line NIH/hmcy1). The nuclear DNA of *c-myc*-transformed cells was digested at a faster rate (1.7-fold for accumulation of mono- and dinucleosome sized DNA fragments) than that of the parental NIH-3T3 cells (data not shown). Thus, in agreement with Laitinen *et al.* (1990, 1995), these observations provided evidence consistent with the observation that *ras*- and *c-myc*-transformed mouse fibroblasts have a less condensed chromatin structure than the parental cells.**

***ras*-Transformed Mouse Fibroblasts Have Elevated Levels of Phosphorylated H1—H1 is responsible for the stabilization of the higher order structure of chromatin. A significant reduction in the content of H1 in *ras*-transformed cells might result in a less condensed chromatin than that of the parental cell chromatin.**

Fig. 1, C and D, shows, however, that the chromatin of parental and *ras*-transformed mouse fibroblasts (Ciras-2) had similar amounts of H1 relative to the core histones (histones H2A, H2B, H3, and H4). Thus, these data suggest that differences in the chromatin structure of oncogene-transformed and parental mouse fibroblasts is not due to a change in the level of H1.

Changes in the content of H1 subtypes and/or modified histone H1 isoforms could account for the observed alterations in chromatin compaction (Laitinen *et al.*, 1995). Thus, we next investigated the level of H1 subtypes and H1-modified forms in nuclei from cells. H1 was isolated by perchloric acid extraction from the nuclei of mouse 10T $\frac{1}{2}$ fibroblasts and transformed derivatives of these cells (Ciras-2, Ciras-3) and resolved by two-dimensional polyacrylamide gel electrophoresis (SDS by AUT), which separates H1 subtypes and their phosphorylated isoforms. Using the nomenclature of Lennox *et al.* (1982), Fig. 2, A, B, and C, shows that H1 subtypes H1b, -d, -e, -c, and H1⁰ were present in both *ras*-transformed and parental 10T $\frac{1}{2}$ mouse fibroblast nuclei; subtype H1a was absent. Densitometric scans of the H1 subtypes resolved on SDS gels demonstrated that the relative levels of the H1 subtypes were similar in *ras*-transformed and parental 10T $\frac{1}{2}$ fibroblasts (data not shown). For example, the relative amount of H1⁰ in the H1 population in the cell lines 10T $\frac{1}{2}$, Ciras-2, and Ciras-3 was comparable.

Lennox and Cohen (1988b) have shown that some of mouse H1 subtypes (H1b and H1c) undergo two types of phosphorylation. One phosphorylated isoform has an altered mobility in SDS gels. This type of phosphorylation is called c-phosphorylation because of its effect on protein conformation. The other phosphorylated isoform retains the same mobility as the parent band. The c-phosphorylated isoforms of H1 subtypes H1b and H1c migrate slower than the unmodified H1 subtype on SDS gels. Fig. 2A shows that H1 from *ras*-transformed cell nuclei had greater amounts of an H1 isoform (c-pb) running slower than H1b and an isoform (c-pc) migrating between H1c and H1d or -e on SDS gels. Consistent with these bands corresponding to the c-phosphorylated isoforms, treatment of H1 with alkaline phosphatase resulted in reduction or disappearance of these bands (Fig. 3C). The amounts of the c-phosphorylated H1b and H1c were approximately 2- to 3-fold greater in the *ras*-transformed cells (Fig. 2A and Table I). These observations provided evidence that the level of the phosphorylated H1 was elevated in *ras*-transformed cells.

To gain further evidence that H1 of *ras*-transformed and parental mouse fibroblasts were differentially phosphorylated, cells were metabolically labeled with [³²P]orthophosphate, and H1 was electrophoretically resolved on SDS-polyacrylamide gels. H1 of parental 10T $\frac{1}{2}$ cells was labeled to lower levels than

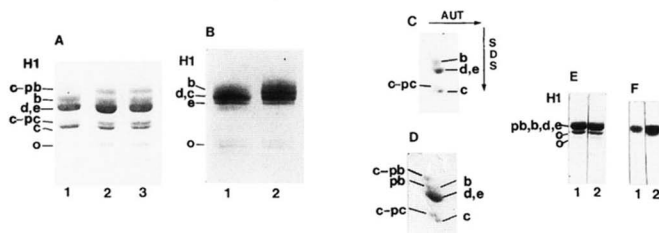


FIG. 2. H1 of *ras*-transformed and parental mouse fibroblasts. H1 was isolated from 10T½ (lane 1), Ciras-2 (lane 2), and Ciras-3 (lane 3) mouse fibroblasts. H1 (2 µg) was electrophoretically resolved on SDS (A) (10T½, lane 1; Ciras-2, lane 2; Ciras-3, lane 3), AUT (B) (10T½, lane 1; Ciras-2, lane 2), or two-dimensional gels (AUT into SDS) (10T½, C; Ciras-2, D). E and F, H1 (2 µg) extracted from 10T½ (lane 1) and Ciras-2 (lane 2) cells metabolically labeled with [³²P]orthophosphate were electrophoretically separated on SDS-15% polyacrylamide gels. On this gel, c-pb and c-pc were not resolved from b and c, respectively. E shows the Coomassie Blue-stained gel, and F shows the accompanying autoradiogram. pb is the phosphorylated isoform of H1b. c-pb and c-pc are the c-phosphorylated isoforms of H1b and H1c, respectively.

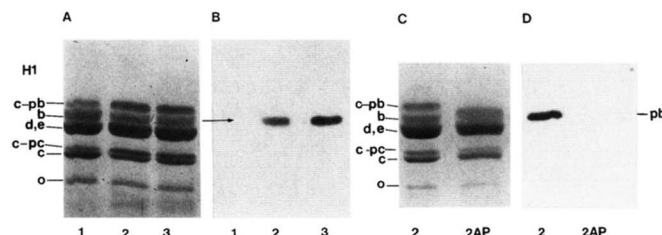


FIG. 3. Phosphorylated H1 subtypes of *ras*-transformed and parental mouse fibroblasts. H1 (2 µg) isolated from 10T½ (lane 1), Ciras-2 (lane 2), or Ciras-3 (lane 3) was resolved on SDS-15% polyacrylamide gels. A and C show the India ink-stained patterns of H1 transferred to the membranes. The membranes shown in B and D were immunochemically stained with the antiphosphorylated H1 antibody as described under "Materials and Methods." C and D, the Ciras-2 H1 were treated with alkaline phosphatase (lane 2AP). pb, c-pb, and c-pc are the phosphorylated isoforms of H1b and c-phosphorylated isoforms of H1b and H1c, respectively.

TABLE I
*Distribution of the *ras*-transformed and parental 10T½ cells in the various phases of the cell cycle and relative content of phosphorylated H1 subtypes*

The percentage of cells in each cell cycle phase is shown. These cells were used to isolate H1 analyzed by SDS-polyacrylamide gel electrophoresis (Fig. 2) and by Western blot analysis with an antiphosphorylated H1 antibody (Fig. 3). The level of the phosphorylated H1 subtype in the *ras*-transformed cells compared to that in the parent 10T½ cells was determined as described under "Materials and Methods."

Cell line	Cell cycle phase			Relative level of phosphorylated H1 subtype		
	G ₁	S	G ₂ /M	c-pH1b	pH1b	c-pH1c
% distribution						
10T½	59	16	25	1.0	1.0	1.0
Ciras-2	44	34	22	2.8	3.8	1.9
Ciras-3	65	22	13	2.8	4.2	2.0

the H1 isolated from *ras*-transformed mouse fibroblasts (Ciras-2) (Fig. 2, E and F). Densitometric scanning of autoradiograms of labeled H1 resolved on SDS gels indicated that labeling of H1 from the highly metastatic Ciras-2 cell line was approximately 5-fold higher than that of the H1 from the normal parental 10T½ cell line.

Previous studies have shown that the level of phosphorylation of H1 varies considerably during the cell cycle. Possibly, a greater percentage of the *ras*-transformed mouse fibroblasts were in S and G₂/M phases of the cell cycle than that of the parental cells. The proportion of cells in the different phases of the cell cycle was determined by flow cytometry of cells stained with ethidium bromide (Table I). The *ras*-transformed cells had

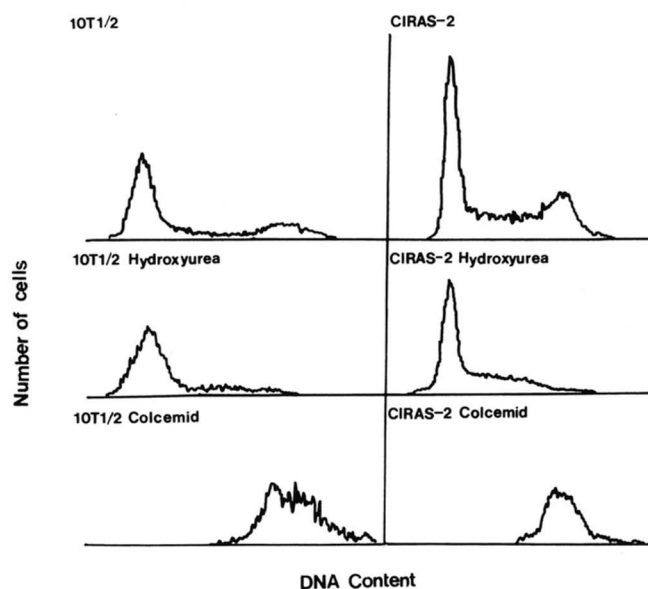


FIG. 4. Effect of hydroxyurea or colcemid on cell cycle progression of *ras*-transformed and parental mouse fibroblasts. Parental 10T½ cells and Ciras-2 cells were either untreated (top panels) or treated with 2 mM hydroxyurea for 24 h (middle panels) or with 0.06 µg/ml colcemid for 16 h (bottom panels) as described under "Materials and Methods." DNA content in the ethidium bromide-stained cells was determined by flow cytometry. The number of cells is represented on the y axis, and the amount of DNA (fluorescence intensity) is shown on the x axis.

less cells in the G₂/M phase of the cell cycle, where H1 phosphorylation is at its peak, than did the parental cells. Further, the Ciras-3 cells had a greater percentage of the cell population in G₁ than did the parental cell line. It is clear, therefore, that the increased level of H1 phosphorylation in the *ras*-transformed cells was not due to a change in the proportion of these cells in S and G₂/M.

The Level of the Phosphorylated Isoform of Histone H1b Is Elevated in *ras*-Transformed Cells—Recently, a novel antibody was generated against a hyperphosphorylated isoform of *Tetrahymena* macronuclear H1 (Lu *et al.*, 1994). This antibody is highly selective for the phosphorylated isoforms of human and *Tetrahymena* H1. Using H1 isolated from the *ras*-transformed and parental 10T½ mouse fibroblast cell lines, the antiphosphorylated H1 antibody detected only one of the phosphorylated H1 subtypes (histone H1b) resolved by SDS-polyacrylamide (Fig. 3B) and two-dimensional gel electrophoresis (not shown). Interestingly, the phosphorylated H1b species recognized by this antibody comigrated with the unmodified parental band on SDS gels, while the c-phosphorylated isoform of histone H1b was not detected by the antibody. However, incubation of H1 with alkaline phosphatase prior to gel electrophoresis and blotting negated the ability of the antibody to detect any of the H1 subtypes (Fig. 3D).

The level of the phosphorylated H1b isoform in *ras*-transformed and parental 10T½ cell lines was determined in Western blot experiments with the antiphosphorylated H1 antibody. Fig. 3B shows the abundance of phosphorylated H1b was greater in the *ras*-transformed cells (Ciras-2 and Ciras-3) than in the parental 10T½ cells. The *ras*-transformed cells had an approximate 4-fold increase in the amount of phosphorylated H1b (Table I). Similar results were obtained when H1 was acid-extracted directly from the cells.

ras-transformed Ciras-2 cells treated with colcemid, which arrests cells at mitosis (Fig. 4), had high levels of hyperphosphorylated histones (data not shown, see Lu *et al.* (1994)). Although phosphorylation of H1 subtypes should be maximal

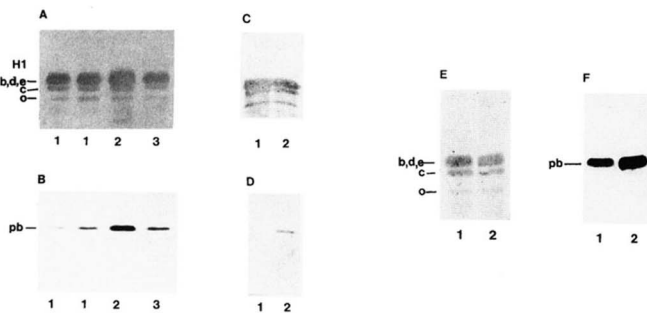


FIG. 5. Immunoblot analysis of phosphorylated H1 isoforms of normal and ras-transformed mouse fibroblasts treated with hydroxyurea or colcemid. Cells (10T½, lane 1; Ciras-2, lane 2; R2, lane 3) were treated with hydroxyurea (A–D) or colcemid (E and F) as described in the legend to Fig. 4. H1 was resolved on SDS-15% polyacrylamide gels and then transferred to membranes which were immunochemically stained for phosphorylated H1. The amount of protein loaded in each lane was as follows: A from left to right: lane 1, 10T½, 1.5 μ g; lane 1 (second), 10T½, 2.0 μ g; lane 2, Ciras-2, 2.0 μ g; lane 3, R2, 1.5 μ g. C: lane 1, 10T½, 2 μ g; lane 2, Ciras-2, 2.0 μ g. E, H1 histones (2 μ g) were isolated from Ciras-2 cells that were not treated (lane 1) or treated (lane 2) with colcemid. A, C, and E show membranes stained with India ink, and B, D, and F show the corresponding immunochemically stained membranes. pb is phosphorylated H1b.

in mitotically arrested Ciras-2 cells, the antiphosphorylated H1 antibody still detected only the phosphorylated H1b isoform (Fig. 5). Thus, it appears that the antiphosphorylated H1 antibodies are remarkably specific for the H1b isoform.

ras-Transformed Cells in the G₁/S Phase of the Cell Cycle Have Elevated Amounts of Phosphorylated H1b—Analysis of the proportion of cells in the different phases of the cell cycle showed that the cell cycle distributions of the ras-transformed and parental cells were similar (Table I). Thus, the elevated levels of the phosphorylated isoform of H1b in ras-transformed cells could not be accounted for by a greater percentage of the ras-transformed cells being in the S or G₂/M phases of the cell cycle. These observations suggested that G₁/S phase ras-transformed cells had a higher amount of phosphorylated H1 than parental 10T½ cells. To determine the level of phosphorylated H1 in G₁/S phase, 10T½, Ciras-2, and R2 (ras-transformed mouse 10T½ fibroblasts that are tumorigenic but not metastatic), cells were treated with the DNA synthesis inhibitor, hydroxyurea, which arrests cells in G₁/S phase of the cell cycle (Ashihara and Baserga, 1979), due to an inhibition of ribonucleotide reductase (McClarty *et al.*, 1990). Following treatment of cells with hydroxyurea, the distribution of cells in the G₁, S, and G₂/M phases of the cell cycle was determined. Fig. 4 shows that hydroxyurea-treated cells had few cells in G₂/M, with the majority of the cells being in G₁ (73% for 10T½; 68% for Ciras-2). Western blot analysis of the H1 isolated from hydroxyurea-treated 10T½, R2, and Ciras-2 cells with the antiphosphorylated H1 antibody showed that the ras-transformed cell lines had higher levels (3–4-fold) of phosphorylated H1b compared to the parental cells (Fig. 5; Table II). The amounts of c-phosphorylated H1b and H1c were also greater in the ras-transformed cells than in the parental cells (Table II).

Phosphorylation of Histone H1 in Cell Lines Transformed with Oncogenes Encoding Protein Kinases—Oncogenic ras can lead to the persistent activation of the MAP kinase pathway. In this pathway, activated Ras activates Raf, a protein-serine kinase, which in turn activates MAP kinase kinase and then MAP kinase (Avruch *et al.*, 1994; Lange-Carter and Johnson, 1994). MAP kinases stimulate the activity of transcription factors (e.g. c-Myc), leading to the induction of cyclins and activation of cyclin-dependent protein kinases, some of which phosphorylate H1 (Jansen-Durr *et al.*, 1993; Hunter and Pines, 1994; Filmus *et al.*, 1994; Daksis *et al.*, 1994). Possibly persist-

TABLE II
Relative level of phosphorylated H1 subtypes in hydroxyurea-arrested 10T½ and ras-transformed mouse fibroblasts

The cell lines 10T½, Ciras-2, and R-2 cells were treated with hydroxyurea. The H1 were resolved on SDS gels, and the level of phosphorylated H1 on Coomassie Blue-stained gel patterns or Western blots (shown in Fig. 5B) was determined as described under "Materials and Methods."

Cell line	Relative level of phosphorylated H1 subtype		
	c-pH1b	pH1b	c-pH1c
10T½	1.0	1.0	1.0
Ciras-2	1.7	4.0	1.3
R-2	1.9	3.1	1.3

ent activation of the MAP kinase pathway leads to the increased phosphorylation of H1. To test this idea, we studied the phosphorylation level of H1 in cells transformed with kinase oncogenes *mos*, *raf*, and *fes* (Egan *et al.*, 1987b), which act upon the MAP kinase pathway. Levels of phosphorylated H1 subtypes in an NIH-3T3 cell line transformed with *c-myc*, a target of the MAP kinases, were also analyzed. Table III shows that the cell cycle distributions of the parental and oncogene-transformed NIH-3T3 mouse fibroblasts were closely matched, although the oncogene-transformed cells tended to have more cells in G₁. The relative levels of the H1 subtypes H1b, -d, -e, and -c appeared to be similar for the parent and oncogene-transformed cell lines. However, the level of H1⁰ in the oncogene-transformed cells was lower than in the parental NIH-3T3 fibroblasts (Fig. 6A). Densitometric scanning of the Coomassie Blue-stained SDS-polyacrylamide gel containing the H1 samples showed that the content of H1⁰ in the oncogene-transformed cells was reduced to approximately 47% of the H1⁰ levels of parental cells. This observation is consistent with the results obtained by Laitinen *et al.* (1995). In addition to a change in the content of H1⁰, the oncogene-transformed cells had elevated levels of the c-phosphorylated isoforms of H1b and H1c (Fig. 6A) and phosphorylated H1b (Fig. 6B). The content of the phosphorylated isoforms of H1b and H1c was elevated 2–4-fold in all of the oncogene-transformed cells (Table III).

Recently, Mansour *et al.* (1994) demonstrated that constitutively active MAP kinase kinase transformed NIH-3T3 mouse fibroblasts. Fig. 7 shows the content of H1 subtypes and their phosphorylated isoforms in the parental NIH-3T3, K97M (cells transfected with catalytically inactive MAP kinase kinase), and Δ N3S222D (cells transfected with constitutively active MAP kinase kinase). Densitometric scanning of the Coomassie Blue-stained SDS gels indicated that the Δ N3S222D cells had slightly higher amounts of c-phosphorylated H1b than the parental or K97M cell lines. Differences in the levels of the H1 subtypes including H1⁰ were not observed. In Western blot analysis of the level of phosphorylated H1b in the H1 preparations, the content of this phosphorylated H1 isoform was found to be highest in the H1 from Δ N3S222D cells (Fig. 7B and Table III). For the Western blot shown in Fig. 7, the antiphosphorylated H1 antibody detected two bands. However, in two repeats of this Western blot experiment, only one band was immunologically stained.

Immunolocalization of Phosphorylated Histone H1b in ras-Transformed and Normal 10T½ Mouse Fibroblasts—Lu *et al.* (1994) demonstrated that antiphosphorylated H1 antibodies did not stain the nuclei of unsynchronized HeLa cells equivalently. HeLa cells in the G₁ phase of the cell cycle were weakly stained and exhibited a punctate pattern of staining. Cells in the S phase had a uniform, more intense staining but less than the staining observed for G₂/M phase cells. Thus, the staining intensity of the nuclei in the various phases of the cell cycle agreed with the biochemical data on changes in H1 phospho-

TABLE III

Cell cycle distribution and level of phosphorylated H1 of NIH-3T3 mouse fibroblasts and NIH-3T3 cells transformed with *fes*, *mos*, *myc*, *raf*, or constitutively active MAP kinase kinase

The H1 histones isolated from the oncogene- or MAP kinase kinase-transformed and parental NIH-3T3 cell lines were resolved on SDS gels, and the level of phosphorylated H1 histones on Coomassie Blue-stained gel patterns or Western blots (shown in Figs. 6 and 7) was determined as described under "Materials and Methods."

Cell line	Cell cycle phase			Relative level of phosphorylated H1 subtype		
	G ₁	S	G ₂ /M	c-pH1b	pH1b	c-pH1c
% distribution						
NIH-3T3	35	36	28	1.0	1.0	1.0
<i>fes</i>	43	26	31	2.3	3.5	2.4
<i>mos</i>	42	41	16	2.6	1.9	2.2
<i>myc</i>	56	24	21	2.6	3.5	2.4
<i>raf</i>	47	27	26	2.8	1.7	1.8
NIH-3T3	69	20	12	1.0	1.0	1.0
K97	69	19	13	1.0	0.6	0.8
ΔN3S222D	67	18	15	1.1	3.7	1.0

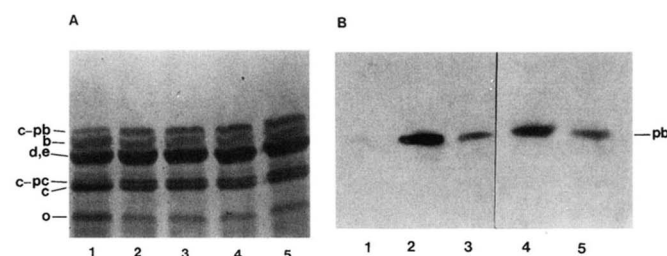


FIG. 6. Phosphorylated H1 isoforms of parental and oncogene-transformed NIH-3T3 mouse fibroblasts. H1 (2 μ g) isolated from NIH-3T3 cells (lane 1) or NIH-3T3 cells transformed with *v-fes* (lane 2), *v-mos* (lane 3), *c-myc* (lane 4), or *A-raf* (lane 5). H1 was resolved on SDS-15% polyacrylamide gels, transferred to membranes which were stained with India ink (A) and then immunochemically stained with antiphosphorylated H1 antibody (B). *pb* is phosphorylated H1b. *c-pb* and *c-pc* are the c-phosphorylated isoforms of H1b and H1c, respectively.

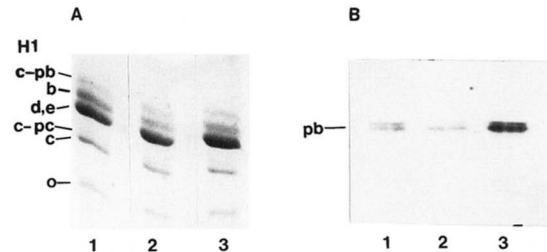


FIG. 7. Phosphorylated H1 of NIH-3T3 cells transformed with constitutively active MAP kinase kinase. H1 isolated from NIH-3T3 cells (lane 1), K97M (NIH-3T3 cells transfected with inactive MAP kinase kinase, lane 2), Δ N3S222D (NIH-3T3 cells transfected and transformed with constitutively active MAP kinase kinase, lane 3). H1 (2 μ g) was resolved on SDS-15% polyacrylamide gels, transferred to membranes which were stained with India ink (A) and then immunochemically stained with antiphosphorylated H1 antibody (B). *pb* is phosphorylated H1b. *c-pb* and *c-pc* are the c-phosphorylated isoforms of H1b and H1c, respectively.

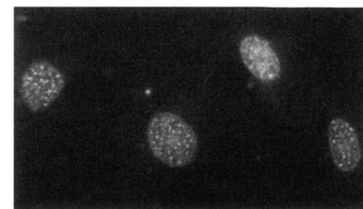
ylation during the mammalian cell cycle.

Before staining *ras*-transformed and parental 10T $\frac{1}{2}$ cells with the antiphosphorylated H1 antibody, we ascertained the specificity of the antiphosphorylated H1 antibody using total cellular protein from Ciras-2 cells. Western blot analysis indicated that the antibody detected only the phosphorylated H1b isoform in total protein.² Cells growing on coverslips were fixed, and the phosphorylated H1b isoform was localized by

10T $\frac{1}{2}$

ANTI-PHOS H1

A

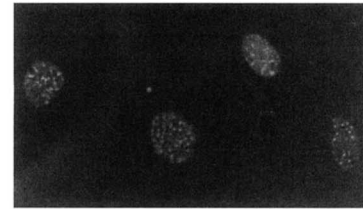


B



B1C8

C



D

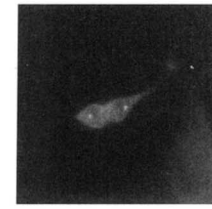


FIG. 8. Phosphorylated H1b colocalizes with the B1C8 nuclear matrix antigen in 10T $\frac{1}{2}$ mouse fibroblast nuclei. Cells were fixed on coverslip and double-stained by indirect immunofluorescence with antiphosphorylated H1 antibody and B1C8 monoclonal antibody and then goat anti-rabbit antibody conjugated to fluorescein isothiocyanate (A and B) and goat anti-mouse antibody conjugated to Texas red (C and D). The immunochemically stained 10T $\frac{1}{2}$ cells were photographed at $\times 60$ magnification. B and D show a cell in M phase of the cell cycle.

indirect immunofluorescence using the antiphosphorylated H1 antibody. The majority of the interphase 10T $\frac{1}{2}$ and *ras*-transformed (Ciras-2) cells had a weak nuclear fluorescence and punctate fluorescent dots dispersed throughout the nucleoplasm (Figs. 8 and 9). The staining of the Ciras-2 nuclei was more diffuse than the 10T $\frac{1}{2}$ nuclei. This was probably due to cell and nuclei shape. The 10T $\frac{1}{2}$ cells were flat and their nuclei large, while the Ciras-2 cells were round and their nuclei appeared smaller. The number of speckles observed for *ras*-transformed and parental cells were equivalent. Occasionally, we observed cells that were in M phase (see Fig. 8B). As might be expected, the mitotic chromosomes stained intensely for phosphorylated H1.

The punctate/speckled pattern of nuclear staining observed with this antibody (also see Lu *et al.*, 1994) is reminiscent of the finding that nuclear sites of splicing factors, small nuclear RNAs, and RNA synthesis were colocalized (Huang and Spector, 1991, 1992; Carter *et al.*, 1991; Bassim-Hassan *et al.*, 1994; Jackson *et al.*, 1993). To ascertain whether the phosphorylated H1b was colocalizing with the sites of splicing factors and "transcript domains" (Xing *et al.*, 1993), the monoclonal antibody B1C8 was also used in indirect immunolocalization studies. The B1C8 monoclonal antibody recognizes a 180-kDa human nuclear matrix protein and co-immunoprecipitates exon-containing RNA from *in vitro* splicing reactions (Wan *et al.*, 1994; Blencowe *et al.*, 1994). Western blot experiments with the B1C8 monoclonal antibody and total protein isolated from 10T $\frac{1}{2}$ mouse fibroblasts showed that the monoclonal antibody detected a 180-kDa mouse protein.² The relative nuclear positioning of phosphorylated H1b and the B1C8 antigens was done by double staining with antiphosphorylated H1b rabbit antibody and B1C8 mouse monoclonal antibody. Figs. 8 and 9 show that the majority of the speckles in the nuclei of 10T $\frac{1}{2}$ and Ciras-2 cells observed with the antiphosphorylated H1 antibody were detected with the B1C8 monoclonal antibody. Of the 40 to 50 speckles illuminated by the antibodies, approximately 80% overlapped. Thus, phosphorylated H1b appeared to be

² D. N. Chadee, W. R. Taylor, R. A. R. Hurta, C. D. Allis, J. A. Wright, and J. R. Davie, unpublished observations.

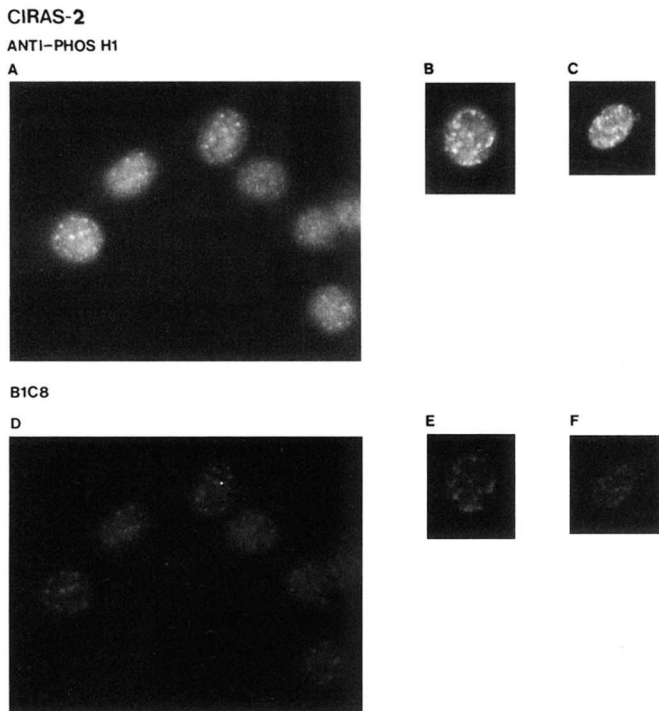


FIG. 9. Phosphorylated H1b colocalizes with the B1C8 nuclear matrix antigen in Ciras-2 mouse fibroblast nuclei. Ciras-2 cells were fixed on the surface of a coverslip and stained by indirect immunofluorescence with antiphosphorylated H1 antibody and B1C8 monoclonal antibody and then goat anti-rabbit antibody conjugated to fluorescein isothiocyanate (A, B, and C) and goat anti-mouse antibody conjugated to Texas red (D, E, and F). The immunocytochemically stained Ciras-2 cells were photographed at $\times 60$ magnification.

localized to sites of RNA processing and gene transcription in the majority of the interphase 10T½ and *ras*-transformed cells. However, for cells in mitosis, the B1C8 staining did not colocalize with the staining for phosphorylated H1b, where intense staining of B1C8 was found at the spindle poles (see Fig. 8D). This pattern of redistribution of the B1C8 antigen during mitosis in mouse fibroblasts is similar to that observed in human CaSki cells (Wan *et al.*, 1994).

DISCUSSION

ras- and *c-myc*-transformed mouse fibroblasts (NIH-3T3 and 10T½) have a less condensed chromatin structure than the parental cell line (this report; Laitinen *et al.* (1990, 1995)). Since H1 stabilizes higher order chromatin structure, it was reasonable to suggest that changes in H1 would be a factor in chromatin decondensation. Alterations in H1 subtypes have been observed in transformed cells (Tan *et al.*, 1982; Davie and Delcave, 1991; Nagaraja *et al.*, 1995). A reduction in the content of H1⁰ in *ras*-transformed NIH-3T3 mouse fibroblasts may contribute to the decondensation of the chromatin in the *ras*-, *raf*-, *fes*-, *mos*-, and *myc*-transformed cells (Laitinen *et al.* (1995) and references therein). However, the lower level of histone H1⁰ in oncogene-transformed mouse fibroblasts was not a general observation. *ras*-transformed 10T½ mouse fibroblasts and constitutively active MAP kinase kinase-transformed NIH-3T3 cells had a content of H1 subtypes (including H1⁰) that was similar to that of parental cells.

The one consistent alteration we observed in the oncogene-transformed 10T½ and NIH-3T3 mouse fibroblasts was an increase in the level of phosphorylated H1 subtypes. The content of phosphorylated H1b and H1c that have a reduced mobility on SDS gels was elevated in the oncogene-transformed cells. Furthermore, in Western blot experiments with an antibody that is highly selective for the phosphorylated form of H1b

in these cells, we found that the level of this phosphorylated subtype was increased in all oncogene-transformed cells used in this study. Similar results were obtained when the levels of phosphorylated H1b and the c-phosphorylated isoforms of H1c and H1b were analyzed from cells transformed with combinations of *ras*, *myc*, and mutant p53 (data not shown).

Studies with native and reconstituted chromatin show that phosphorylated H1 destabilize chromatin structure (Kaplan *et al.*, 1984; Hill *et al.*, 1991). Further, in studies with avian fibroblasts transfected with H5 (an H1 variant), H5 was shown to inhibit proliferation in normal fibroblasts but not in transformed cells, in which H5 was phosphorylated. Aubert *et al.* (1991) proposed that phosphorylated H5 lacked the ability to condense chromatin. Thus, these and other studies (see Lu *et al.* (1994) and references therein) provide support for the idea that an increase in the phosphorylation of H1 leads to destabilization of the chromatin in oncogene-transformed cells.

Mouse fibroblasts transformed with *raf*, *fes*, or *mos* had elevated levels of phosphorylated H1 subtypes. These oncogenes code for serine/threonine or tyrosine kinases and act upon the MAP kinase signal transduction pathway (Hunter and Pines, 1994). NIH-3T3 cells transformed with constitutively active MAP kinase kinase also had an increased content of phosphorylated H1b and, to a lesser extent, c-phosphorylated H1b. These observations suggest that persistent activation of the MAP kinase pathway has a role in the intensified phosphorylation of H1 in the transformed cells. One of the downstream targets of the MAP kinase pathway is the c-Myc protooncogene product. Phosphorylation of c-Myc increases its ability to transactivate genes (Davis, 1993). Myc and activated Ras enhance the expression of cyclins D1, E, and A (Jansen-Durr *et al.*, 1993; Daksis *et al.*, 1994; Filmus *et al.*, 1994). Overexpression of cyclin E in cells significantly enhances cyclin E-associated H1 kinase activity (Resnitzky *et al.*, 1994). It is possible that activation of the MAP kinase signal transduction pathway leads to the phosphorylation of c-Myc which in turn increases the expression of cyclins E and A and activity of a cyclin E- or cyclin A-associated H1 kinase (Jansen-Durr *et al.*, 1993; Hunter and Pines, 1994).

The high selectivity of the antiphosphorylated H1 antibody allowed us to ascertain the cellular location of the phosphorylated isoform of H1b. A punctate pattern of nuclear staining of *ras*-transformed and parental 10T½ cells was observed. Clearly, the results show that the phosphorylated isoform of H1b is non-uniform in the nuclei of parental and *ras*-transformed mouse fibroblasts. In M-phase cells, the punctate pattern of staining is lost, and an intense staining of the mitotic chromosomes is observed. A similar staining was observed for non-S phase HeLa nuclei (Lu *et al.*, 1994).

The speckled pattern observed with the antiphosphorylated H1 antibody closely matched the pattern found with the B1C8 monoclonal antibody. B1C8 colocalizes with other RNA splicing components (SC35, snRNPs) (Blencowe *et al.*, 1994). Several transcribed genes (e.g. *c-fos*) have been located near sites containing the RNA splicing components (Huang and Spector, 1991; Carter *et al.*, 1993; Xing *et al.*, 1993). Furthermore, the punctate pattern of splicing factors is sensitive to inhibitors of transcription (Huang *et al.*, 1994). Recently, Durfee *et al.* (1994) found that the nuclear matrix protein p84, which is present in human and mouse cells and binds to the N-terminal domain of dephosphorylated Rb, colocalizes with the B1C8 antigen. Dephosphorylated Rb binds to the transcription factor E2F, which is involved in the activation of several early response genes, including *c-myc*. Although inactive when bound to dephosphorylated Rb, E2F still has the capacity to bind its target DNA (Nevins, 1992; Weintraub *et al.*, 1992). Thus, the nuclear ma-

trix-bound p84, which is near sites containing splicing factors, through its association with dephosphorylated Rb-E2F complex, may attract early response genes to sites of RNA processing. Following the release of E2F from Rb, E2F forms a complex with cyclin E (and later with A), p107, and CDK2 (Hunter and Pines, 1994). It is an attractive hypothesis that the transcription factor E2F directs the H1 kinase activity of CDK2 to transcriptionally active chromatin regions (Devoto *et al.*, 1992).

REFERENCES

Ashihara, T., and Baserga, R. (1979) *Methods Enzymol.* **58**, 248–262

Aubert, D., Garcia, M., Benchaib, M., Poncet, D., Chebloune, Y., Verdier, G., Nigon, V., Samarut, J., and Mura, C. V. (1991) *J. Cell Biol.* **113**, 497–506

Avruch, J., Zhang, X.-F., and Kyriakis, J. M. (1994) *Trends Biochem. Sci.* **19**, 279–283

Bassim-Hassan, A., Errington, R. J., White, N. S., Jackson, D. A., and Cook, P. R. (1994) *Cell Sci.* **107**, 425–434

Belikov, S. V., Belgovsky, A. I., Preobrazhenskaya, O. V., Karpov, V. L., and Mirzabekov, A. D. (1993) *Nucleic Acids Res.* **21**, 1031–1034

Blencowe, W. J., Nickerson, J. A., Issner, R., Penman, S., and Sharp, P. A. (1994) *J. Cell Biol.* **127**, 593–607

Blosmanis, R., Wright, J. A., and Goldenberg, G. J. (1987) *Cancer Res.* **47**, 1273–1277

Blumer, K. J., and Johnson, G. L. (1994) *Trends Biochem. Sci.* **19**, 236–240

Bradbury, E. M. (1992) *BioEssays* **14**, 9–16

Breneman, J. W., Yau, P., Teplitz, R. L., and Bradbury, E. M. (1993) *Exp. Cell. Res.* **206**, 16–26

Carter, K. C., Taneja, K. L., and Lawrence, J. B. (1991) *J. Cell Biol.* **115**, 1191–1202

Carter, K. C., Bowman, D., Carrington, W., Fogarty, K., McNeil, J. A., Fay, F. S., and Lawrence, J. B. (1993) *Science* **259**, 1330–1335

Cole, R. D. (1987) *Int. J. Peptide Protein Res.* **30**, 433–449

Daksis, J. I., Lu, R. Y., Facchini, L. M., Marhin, W. W., and Penn, L. J. Z. (1994) *Oncogene* **9**, 3635–3645

Davie, J. R. (1982) *Anal. Biochem.* **120**, 276–281

Davie, J. R., and Delcuve, G. P. (1991) *Biochem. J.* **280**, 491–497

Davie, J. R., Delcuve, G. P., Nickel, B. E., Moirier, R., and Bailey, G. (1987) *Cancer Res.* **47**, 5407–5410

Davis, R. J. (1993) *J. Biol. Chem.* **268**, 14553–14556

Delcuve, G. P., and Davie, J. R. (1989) *Biochem. J.* **263**, 179–186

Delcuve, G. P., and Davie, J. R. (1992) *Anal. Biochem.* **200**, 339–341

Devoto, S. H., Mudryj, M., Pines, J., Hunter, T., and Nevins, J. R. (1992) *Cell* **68**, 167–176

Durfee, T., Mancini, M. A., Jones, D., Elledge, S. J., and Lee, W. -H. (1994) *J. Cell Biol.* **127**, 609–622

Egan, S. E., McClarty, G. A., Jarolim, L., Wright, J. A., Spiro, I., Hager, G., and Greenberg, A. H. (1987a) *Mol. Cell. Biol.* **7**, 830–837

Egan, S. E., Wright, J. A., Jarolim, L., Yanagihara, K., Bassin, R. H., and Greenberg, A. H. (1987b) *Science* **238**, 202–205

Ericsson, C., Grossbach, U., Bjorkroth, B., and Daneholt, B. (1990) *Cell* **60**, 73–83

Filmus, J., Robles, A. I., Shi, W., Wong, M. J., Colombo, L. L., and Conti, C. J. (1994) *Oncogene* **9**, 3627–3633

Garrard, W. T. (1991) *BioEssays* **13**, 87–88

Gorka, C., Fakan, S., and Lawrence, J. J. (1993) *Exp. Cell Res.* **205**, 152–158

Hill, C. S., Packman, L. C., and Thomas, J. O. (1990) *EMBO J.* **9**, 805–813

Hill, C. S., Rimmer, J. M., Green, B. N., Finch, J. T., and Thomas, J. O. (1991) *EMBO J.* **10**, 1939–1948

Hirano, T., and Mitchison, T. J. (1994) *Cell* **79**, 449–458

Hohmann, P. (1983) *Mol. Cell. Biochem.* **57**, 81–92

Huang, S., and Spector, D. L. (1991) *Genes & Dev.* **5**, 2288–2302

Huang, S., and Spector, D. L. (1992) *Proc. Natl. Acad. Sci. U. S. A.* **89**, 305–308

Huang, S., Deerinck, T. J., Ellisman, M. H., and Spector, D. L. (1994) *J. Cell Biol.* **126**, 877–899

Hunter, T., and Pines, J. (1994) *Cell* **79**, 573–582

Jackson, D. A., Hassan, A. B., Errington, R. J., and Cook, P. R. (1993) *EMBO J.* **12**, 1059–1065

Jansen-Durr, P., Meichle, A., Steiner, P., Pagano, M., Finke, K., Botz, J., Wessbecher, J., Draetta, G., and Eilers, M. (1993) *Proc. Natl. Acad. Sci. U. S. A.* **90**, 3685–3689

Kamakaka, R. T., and Thomas, J. O. (1990) *EMBO J.* **9**, 3997–4006

Kaplan, L. J., Bauer, R., Morrison, E., Langan, T. A., and Fasman, G. D. (1984) *J. Biol. Chem.* **259**, 8777–8785

Laitinen, J., Sistonen, L., Alitalo, K., and Holtta, E. (1990) *J. Cell Biol.* **111**, 9–17

Laitinen, J., Sistonen, L., Alitalo, K., and Holtta, E. (1995) *J. Cell. Biochem.* **57**, 1–11

Lange-Carter, C. A., and Johnson, G. L. (1994) *Science* **265**, 1458–1461

Lennox, R. W., and Cohen, L. H. (1983) *J. Biol. Chem.* **258**, 262–268

Lennox, R. W., and Cohen, L. H. (1988a) *Biochem. Cell Biol.* **66**, 636–649

Lennox, R. W., and Cohen, L. H. (1988b) *Histone Genes and Gene Expression*, pp. 375–395, John Wiley and Sons, Inc., New York

Lennox, R. W., Oshima, R. G., and Cohen, L. H. (1982) *J. Biol. Chem.* **257**, 5183–5189

Lin, R., Cook, R. G., and Allis, C. D. (1991) *Genes & Dev.* **5**, 1601–1610

Lu, M. J., Dadd, C. A., Mizzen, C. A., Perry, C. A., McLachlan, D. R., Annunziato, A. T., and Allis, C. D. (1994) *Chromosoma* **103**, 111–121

Mansour, S. J., Matten, W. T., Hermann, A. S., Candia, J. M., Rong, S., Fukasawa, K., Vande Woude, G. F., and Ahn, N. G. (1994) *Science* **265**, 966–979

McClarty, G. A., Chan, A. K., Choy, B. K., and Wright, J. A. (1990) *J. Biol. Chem.* **265**, 7539–7547

Nacheva, G. A., Guschin, D. Y., Preobrazhenskaya, O. V., Karpov, V. L., Ebralidse, K. K., and Mirzabekov, A. D. (1989) *Cell* **58**, 27–36

Nagaraja, S., Delcuve, G. P., and Davie, J. R. (1995) *Biochim. Biophys. Acta* **1260**, 207–214

Nevins, J. R. (1992) *Nature* **358**, 375–376

Nickel, B. E., Roth, S. Y., Cook, R. G., Allis, C. D., and Davie, J. R. (1987) *Biochemistry* **26**, 4417–4421

Ohsumi, K., Katagiri, C., and Kishimoto T. (1993) *Science* **262**, 2033–2035

Parseghian, M. H., Clark, R. F., Hauser, L. J., Dvorkin, N., Harris, D. A., and Hamkalo, B. A. (1993) *Chromosome Res.* **1**, 127–139

Parseghian, M. H., Henscen, A. H., Kriegstein, K. G., and Hamkalo, B. A. (1994a) *Protein Sci.* **3**, 575–587

Parseghian, M. H., Harris, D. A., Rishwain, D. R., and Hamkalo, B. A. (1994b) *Chromosome* **103**, 198–208

Postnikov, Y. V., Shick, V. V., Belyavsky, A. V., Khrapko, K. R., Brodolin, K. L., Nikolskaya, T. A., and Mirzabekov, A. D. (1991) *Nucleic Acids Res.* **19**, 717–725

Resnitzky, D., Gossen, M., Bujard, H., and Reed, S. I. (1994) *Mol. Cell. Biol.* **14**, 1669–1679

Roth, S. Y., and Allis, C. D. (1992) *Trends Biochem. Sci.* **17**, 93–98

Tan, K. B., Borun, T. W., Charpentier, R., Cristofalo, V. J., and Croce, C. M. (1982) *J. Biol. Chem.* **257**, 5337–5338

Van Holde, K. E. (1988) *Chromatin*, Springer-Verlag, New York

Van Holde, K. E., Lohr, D. E., and Robert, C. (1992) *J. Biol. Chem.* **267**, 2837–2840

Wan, K. M., Nickerson, J. A., Krockmalnic, G., and Penman, S. (1994) *Proc. Natl. Acad. Sci. U. S. A.* **91**, 594–598

Weintraub, H. (1984) *Cell* **38**, 17–27

Weintraub, S. J., Prater, C. A., and Dean, D. C. (1992) *Nature* **358**, 259–261

Xing, Y., Johnson, C. V., Dobner, P. R., and Lawrence, J. B. (1993) *Science* **259**, 1326–1330

Yasuda, H., Matsumoto, Y., Mita, S., Marunouchi, T., and Yamada, M. (1981) *Biochemistry* **20**, 4414–4419